IJSES
Volume 9, Issue 1, pp. 71-76, 2025.
International Journal of Scientific Engineering and Science
ISSN (Online): 2456-7361

A High-Order Numerical Method for Fourth-Order Problems in Complex Sector Regions

Ting Dai[1], Jihui Zheng[1,*]
[1]School of Mathematics Science, Guizhou Normal University, Guiyang 550025, China

Abstract— *In this paper, we propose a high-order numerical approach based on a reduced-order scheme for fourth-order problems in complex sector regions. Initially, we introduce an auxiliary variable and construct an affine transformation to convert the fourth-order problem in the complex sector region into an equivalent second-order mixed problem in a standard rectangular domain. In line with the boundary conditions, we introduce a product-type Sobolev space. Subsequently, we derive the variational formulation and discrete scheme for the second-order mixed problem in the standard rectangular domain. Next, by using Legendre basis functions and tensor products, we deduce the equivalent matrix form of the discrete scheme. Finally, we present a series of numerical examples to illustrate the algorithm's convergence and high precision.*

Keywords— *Fourth-order equation; mixed formulation; high-order numerical method; complex sector region*.

I. INTRODUCTION

In scientific research, numerous physical phenomena and chemical reactions, such as the propagation of flames and the heat conduction of materials, can be accurately described using fourth-order equations [1-3]. Numerical computation of differential equations on complex sectorial domains frequently arises in scientific research, and high-precision numerical methods can offer more accurate results for these studies. Currently, the numerical methods commonly utilized for solving fourth-order problems encompass spectral methods [4-6], finite difference methods [7-9], finite element methods [10-12], and finite volume methods [13,14]. For regions with complex curved boundaries, whether employing finite element methods or finite difference methods, boundary approximation not only introduces additional errors, but also significantly increases computational complexity and CPU computation time. As we all know, spectral methods possess the advantage of spectral accuracy. It would be highly meaningful if they could effectively handle the boundary conditions of complex regions while maintaining their high-precision characteristics.

Therefore, this paper aims to propose a high-order numerical approach based on a reduced-order scheme for fourth-order problems in complex sector regions. Initially, we introduce an auxiliary variable and construct an affine transformation to convert the fourth-order problem in the complex sector region into an equivalent second-order mixed problem in a standard rectangular domain. In line with the boundary conditions, we introduce a product-type Sobolev space. Subsequently, we derive the variational formulation and discrete scheme for the second-order mixed problem in the standard rectangular domain. Next, by using Legendre basis functions and tensor products, we deduce the equivalent matrix form of the discrete scheme. Finally, we present a series of numerical examples to illustrate the algorithm's convergence and high precision.

The remainder of this paper is structured as follows: In Section II, we derive an equivalent second-order mixed formulation. In Section III, we introduce a Sobolev space and derive the variational formulation and its discretes cheme. In Section IV, we derive the equivalent matrix form of the discrete scheme. Numerical examples and conclusions are presented in Section V and Section VI, respectively.

II. EQUIVALENT COUPLED SYSTEM

We consider in this paper the following fourth order problem:

$$\Delta^2 H(x,y)-\alpha\Delta H(x,y)+\beta H(x,y)=F(x,y),\ \text{in}\ \Omega, \tag{1}$$

$$H(x,y)=\Delta H(x,y)=0,\ \text{on}\ \partial\Omega, \tag{2}$$

where α and β are non-negative constants, $\Omega\in\mathbb{R}^2$ is a two-dimensional complex sector regions, that is,

$$\Omega=\{(x,y): x=r\hat{R}(\theta)\cos\theta,\ y=r\hat{R}(\theta)\sin\theta, 0<a<r<b, 0\le\theta_1<\theta<\theta_2\le 2\pi\},$$

here $\hat{R}(\theta)>0$ is a function related to θ. Introduce an auxiliary function as follows:

$$G(x,y)=-\Delta H(x,y).$$

Then, (1) and (2) are equivalent to the following second-order mixed formulation:

$$-\Delta H(x,y)-G(x,y)=0, \text{in}\ \Omega, \tag{3}$$

$$-\Delta G(x,y)+\alpha G(x,y)+\beta H(x,y)=F(x,y),\ \text{in}\ \Omega, \tag{4}$$

$$H(x,y)=G(x,y)=0,\ \text{on}\ \partial\Omega. \tag{5}$$

Following [15], through a direct calculation, we obtain that

$$\partial_x^2+\partial_y^2=\frac{1}{r\hat{R}^2}\left\{\left[1+\frac{(\partial_\theta\hat{R})^2}{\hat{R}^2}\right]\frac{\partial}{\partial r}(r\partial_r)-\frac{\partial}{\partial r}\left(\frac{\partial_\theta\hat{R}}{\hat{R}}\partial_\theta\right)-\frac{\partial}{\partial\theta}\left(\frac{\partial_\theta\hat{R}}{\hat{R}}\partial_r\right)+\frac{1}{r}\partial_\theta^2\right\}. \tag{6}$$

Denote

$$\theta=A\xi+B,\ r=C\eta+E,\ \xi\in[-1,1],\eta\in[-1,1],$$

$$A=\frac{\theta_2-\theta_1}{2},\ B=\frac{\theta_2+\theta_1}{2},\ C=\frac{b-a}{2},\ E=\frac{b+a}{2},$$

$$\mathrm{D}=\{(\eta,\xi):-1\le\eta\le1,-1\le\xi\le1\},\ g(\eta,\xi)=G(x,y),$$

$$h(\eta,\xi)=H(x,y),\ R(\xi)=\hat{R}(\theta),\ f(\eta,\xi)=F(x,y).$$

We obtain from (6) that

$$\Delta G(x,y)=\mathrm{L}g(\eta,\xi)=\frac{1}{(C\eta+E)R^2}\left\{\frac{1}{(C\eta+E)A^2}\partial_\xi^2 g-\frac{1}{CA^2}\left[\partial_\eta\left(\frac{\partial_\xi R}{R}\partial_\xi g\right)+\partial_\xi\left(\frac{\partial_\xi R}{R}\partial_\eta g\right)\right]\right.$$

IJSES
Volume 9, Issue 1, pp. 71-76, 2025.
International Journal of Scientific Engineering and Science
ISSN (Online): 2456-7361

$$+\frac{1}{C}\left(1+\frac{1}{A^2}\frac{(\partial_\xi R)^2}{R^2}\right)\left[\partial_\eta g+\left(\eta+\frac{E}{C}\partial_\eta^2 g\right)\right]\Big\}. \quad (7)$$

Then, (1) and (2) can be rewritten as follows:

$$-\mathrm{L}g+\alpha g+\beta h=f,(\eta,\xi)\in \mathrm{D}, \quad (8)$$

$$-\mathrm{L}h-g=0,(\eta,\xi)\in \mathrm{D}, \quad (9)$$

$$h(\eta,\pm 1)=g(\eta,\pm 1)=0,\eta\in[-1,1], \quad (10)$$

$$h(\pm 1,\xi)=g(\pm 1,\xi)=0,\xi\in[-1,1]. \quad (11)$$

III. Sobolev Space and Variational Formulation

In this section, we define a product-type Sobolev space and present the variational formulation and discrete scheme associated with the system of equations (8)-(11). To obtain the variational formulations for the equations in (8)-(11), we first define the following Sobolev spaces:

$$\mathrm{H}_*^1(\mathrm{D})=\Big\{p:\int_{\mathrm{D}}\left(1+\frac{1}{A^2}\frac{(\partial_\xi R)^2}{R^2}\right)|\partial_\eta p|^2-\frac{2}{A}\frac{\partial_\xi R}{R}\partial_\xi p\partial_\eta p$$

$$+|\partial_\xi p|^2\,d\eta d\xi<\infty,\ p(\eta,\pm 1)=0,\ p(\pm 1,\xi)=0\Big\},$$

the corresponding inner product and norm are respectively:

$$(p,q)_{1,*}=\int_{\mathrm{D}}\left(1+\frac{1}{A^2}\frac{(\partial_\xi R)^2}{R^2}\right)\partial_\eta p\partial_\eta q-\frac{1}{A}\frac{\partial_\xi R}{R}(\partial_\xi p\partial_\eta q$$

$$+\partial_\xi q\partial_\eta p)+\partial_\xi p\partial_\xi q d\eta d\xi,$$

$$\|p\|_{1,*}=\left(\int_{\mathrm{D}}|\partial_\eta p|^2+\left|\frac{1}{AR}\partial_\xi R\partial_\eta p-\partial_\xi p\right|^2 d\eta d\xi\right)^{\frac{1}{2}}.$$

By applying Green's formula and integration by parts, the variational formulation of (8)-(11) can be derived as: Find $(h,g)\in \mathrm{H}_*^1(\mathrm{D})\times\mathrm{H}_*^1(\mathrm{D})$ such that

$$\mathrm{A}([h,g],[t,s])=\mathrm{F}([t,s]),\ \forall[t,s]\in \mathrm{H}_*^1(\mathrm{D})\times\mathrm{H}_*^1(\mathrm{D}), \quad (12)$$

where

$$\mathcal{A}([h,g],[t,s])=\int_{\mathcal{D}}\frac{A}{C}(C\eta+E)\Big(1+$$

$$\frac{1}{A^2}\frac{(\partial_\xi R)^2}{R^2}\Big)\partial_\eta h\partial_\eta t d\eta d\xi-\int_{\mathcal{D}}\frac{1}{A}\frac{\partial_\xi R}{R}\partial_\xi h\partial_\eta t d\eta d\xi$$

$$-\int_{\mathrm{D}}\frac{1}{A}\frac{\partial_\xi R}{R}\partial_\xi t\partial_\eta h d\eta d\xi+\int_{\mathrm{D}}\frac{C}{(C\eta+E)A}\partial_\xi h\partial_\xi t d\eta d\xi$$

$$-\int_{\mathrm{D}}AC(C\eta+E)R^2 g t d\eta d\xi+\int_{\mathrm{D}}\frac{C}{(C\eta+E)A}\partial_\xi g\partial_\xi s d\eta d\xi$$

$$+\int_{\mathrm{D}}\frac{A}{C}(C\eta+E)\left(1+\frac{1}{A^2}\frac{(\partial_\xi R)^2}{R^2}\right)\partial_\eta g\partial_\eta s d\eta d\xi-\int_{\mathrm{D}}\frac{1}{A}\frac{\partial_\xi R}{R}\partial_\eta g\partial_\xi s d\eta d\xi$$

$$-\int_{\mathrm{D}}\frac{1}{A}\frac{\partial_\xi R}{R}\partial_\xi g\partial_\eta s d\eta d\xi+\alpha\int_{\mathrm{D}}AC(C\eta+E)R^2 g s d\eta d\xi$$

$$+\beta\int_{\mathrm{D}}AC(C\eta+E)R^2 h s d\eta d\xi,$$

$$\mathrm{F}([t,s])=\int_{\mathrm{D}}AC(C\eta+E)R^2 f s d\eta d\xi.$$

Let P_N be a polynomial space of degree at most N. Define the approximation space: $X_{*N}=(P_N\times P_N)\cap \mathrm{H}_*^1(\mathrm{D})$. Then, a discrete scheme corresponding to (12) is: Find $(h_N,g_N)\in X_{*N}\times X_{*N}$ such that

$$\mathrm{A}([h_N,g_N],[t_N,s_N])=\mathrm{F}([t_N,s_N]),\ \forall[t_N,s_N]\in X_{*N}\times X_{*N}. \quad (13)$$

IV. Effective Implementation of Algorithms

In this section, we aim to construct the matrix form equivalent to the discrete formulation presented in (13). Initially, we denote the i-th Legendre polynomial as $L_i(\xi)$ and let

$$\phi_i(\xi)=L_i(\xi)-L_{i+2}(\xi),\ i=0,1,\cdots,N-2.$$

It is clear that

$$\mathrm{S}_N=\mathrm{span}\{\phi_i(\xi)\phi_j(\eta),\ i,j=0,1,\cdots,N-2\},\ X_{*N}=\mathrm{S}_N\times\mathrm{S}_N.$$

Let us expand g_N and h_N as follows:

$$(g_N,h_N)=\sum_{i,j=0}^{N-2}(w_{ij},u_{ij})\phi_i(\xi)\phi_j(\eta). \quad (14)$$

Setting

$$\mathrm{W}=\begin{pmatrix} w_{00} & w_{01} & \cdots & w_{0\,N-2}\\ w_{10} & w_{11} & \cdots & w_{1\,N-2}\\ \vdots & \vdots & \ddots & \vdots\\ w_{N-2\,0} & w_{N-2\,1} & \cdots & w_{N-2\,N-2}\end{pmatrix},$$

and

$$\mathrm{U}=\begin{pmatrix} u_{00} & u_{01} & \cdots & u_{0\,N-2}\\ u_{10} & u_{11} & \cdots & u_{1\,N-2}\\ \vdots & \vdots & \ddots & \vdots\\ u_{N-2\,0} & u_{N-2\,1} & \cdots & u_{N-2\,N-2}\end{pmatrix}.$$

Let $\bar{\mathbf{w}}$ and $\bar{\mathbf{u}}$ denote the column vectors of length $(N-1)^2$ obtained by expanding W and U respectively along their columns. Denote

$$n_{kj}=\int_{-1}^{1}\frac{A}{C}(C\eta+E)\phi_k'(\eta)\phi_j'(\eta)d\eta,\hat{n}_{kj}$$

$$=\int_{-1}^{1}\left(1+\frac{1}{A^2}\frac{(\partial_\xi R)^2}{R^2}\right)\phi_k(\xi)\phi_j(\xi)d\xi,$$

$$p_{kj}=\int_{-1}^{1}\phi_k'(\eta)\phi_j(\eta)d\eta,\hat{p}_{kj}=\int_{-1}^{1}\frac{1}{A}\frac{\partial_\xi R}{R}\phi_k(\xi)\phi_j'(\xi)d\xi,$$

$$q_{kj}=\int_{-1}^{1}\phi_k(\eta)\phi_j'(\eta)d\eta,\hat{q}_{kj}=\int_{-1}^{1}\frac{1}{A}\frac{\partial_\xi(R)}{R}\phi_k'(\xi)\phi_j(\xi)d\xi,$$

$$z_{kj}=\int_{-1}^{1}\frac{C}{(C\eta+E)A}\phi_j(\eta)\phi_k(\eta)d\eta,\hat{z}_{kj}=\int_{-1}^{1}\phi_k'(\xi)\phi_j'(\xi)d\xi,$$

$$m_{kj}=\int_{-1}^{1}AC(C\eta+E)\phi_k(\eta)\phi_j(\eta)d\eta,\hat{m}_{kj}=\int_{-1}^{1}R^2\phi_k(\xi)\phi_j(\xi)d\xi,$$

$$f_{kl}=\int_{\mathrm{D}}AC(C\eta+E)R^2 f\phi_k(\xi)\phi_l(\eta)d\xi d\eta.$$

By substituting (14) into (13), and then allowing t_N and s_N to traverse a set of basis functions in X_{*N}, respectively, we obtain the equivalent matrix format of (13):

$$\begin{pmatrix} T_1 & -T\\ \beta T_2 & T_1+\alpha T_2\end{pmatrix}\begin{pmatrix}\bar{w}\\ \bar{u}\end{pmatrix}=\begin{pmatrix}0\\ f\end{pmatrix},$$

where $\otimes$ denotes the tensor product, i. e., $A\otimes B=(a_{ij}B)_{ij=0}^{N-2}$ and

$$T_1=N(l,:)\otimes\hat{N}(k,:)-P(l,:)\otimes\hat{P}(k,:)-Q(l,:)$$

$$\otimes\hat{Q}(k,:)+Z(l,:)\otimes\hat{Z}(k,:),$$

International Journal of Scientific Engineering and Science
Volume 9, Issue 1, pp. 71-76, 2025. ISSN (Online): 2456-7361

$$T_2 = M(l, :) \otimes \widehat{M}(k, :), \boldsymbol{f} = (f_{00}, \cdots, f_{N-2,0}; f_{01}, \cdots, f_{N-2,1}; f_{0,N-2}, \cdots, f_{N-2,N-2})^{\mathsf{T}},$$

$$N = (n_{ij})_{ij=0}^{N-2},\ P = (p_{ij})_{ij=0}^{N-2},\ Q = (q_{ij})_{ij=0}^{N-2},\ Z = (z_{ij})_{ij=0}^{N-2},\ M = (m_{ij})_{ij=0}^{N-2},$$

$$\widehat{N} = (\hat{n}_{ij})_{ij=0}^{N-2},\ \hat{P} = (\hat{p}_{ij})_{ij=0}^{N-2},\ \hat{Q} = (\hat{q}_{ij})_{ij=0}^{N-2},\ \hat{Z} = (\hat{z}_{ij})_{ij=0}^{N-2},\ \widehat{M} = (\widehat{m}_{ij})_{ij=0}^{N-2}.$$

V. NUMERICAL EXPERIMENT

In this section, to demonstrate the convergence and effectiveness of the algorithm, a series of numerical experiments will be conducted using MATLAB software, version R2023a. Let $H_N(x,y)$ and $G_N(x,y)$ be the approximate solutions of $H(x,y)$ and $G(x,y)$, respectively. The associated errors are defined as follows:

$$\|H(x,y) - H_N(x,y)\|_{L^2(\Omega)} = \left(\int_{\mathcal{D}} A\, C(C\eta + E) R^2(\xi) |h(\xi,\eta) - h_N(\xi,\eta)|^2 d\xi d\eta \right)^{\frac{1}{2}},$$

$$\|H(x,y) - H_N(x,y)\|_{L^\infty(\Omega)} = \|h(\eta,\xi) - h_N(\eta,\xi)\|_{L^\infty(\mathcal{D})} = \max_{(\eta,\xi)\in\mathcal{D}} |h(\xi,\eta) - h_N(\xi,\eta)|.$$

Example 1: We take $\alpha = \beta = 1, \theta_1 = 0, \theta_2 = \frac{\pi}{2}, a = \frac{1}{2}, b = 1$. Let

$$H(x,y) = x^3 y^3 (x^4 + y^4 - \frac{1}{16})^3 \sin^3((x^4 + y^4)\pi).$$

It is evident that $H(x,y)$ satisfies boundary conditions. By substituting $H(x,y)$ into (1), we obtain $F(x,y)$. We present the errors between the exact solutions $H(x,y)$ and $G(x,y)$ and the approximate solutions $H_N(x,y)$ and $G_N(x,y)$ in Table 1 and Table 2, respectively. Additionally, the comparison diagrams of the exact solution and the approximate solution are presented in Figures 1 and 3. Furthermore, the error images between the exact and approximate solutions are shown in Figures 2 and 4.

TABLE 1. For various values of N, the errors between the exact solution $H(x,y)$ and the approximate solution $H_N(x,y)$.

N	20	30	40	50	60
$\|H(x,y)-H_N(x,y)\|_{L^2}$	8.1173×10^{-7}	4.7202×10^{-9}	2.6113×10^{-11}	1.3986×10^{-13}	4.8145×10^{-15}
$\|H(x,y)-H_N(x,y)\|_{L^\infty}$	1.4215×10^{-6}	8.6137×10^{-9}	4.7131×10^{-11}	2.4663×10^{-13}	5.9137×10^{-15}

TABLE 2. For various values of N, the errors between the exact solution $G(x,y)$ and the approximate solution $G_N(x,y)$.

N	20	30	40	50	60
$\|G(x,y)-G_N(x,y)\|_{L^2}$	0.0017	2.0835×10^{-5}	1.8699×10^{-7}	1.4391×10^{-9}	1.0081×10^{-11}
$\|G(x,y)-G_N(x,y)\|_{L^\infty}$	0.0061	7.3308×10^{-5}	6.6851×10^{-7}	5.2025×10^{-9}	3.7257×10^{-11}

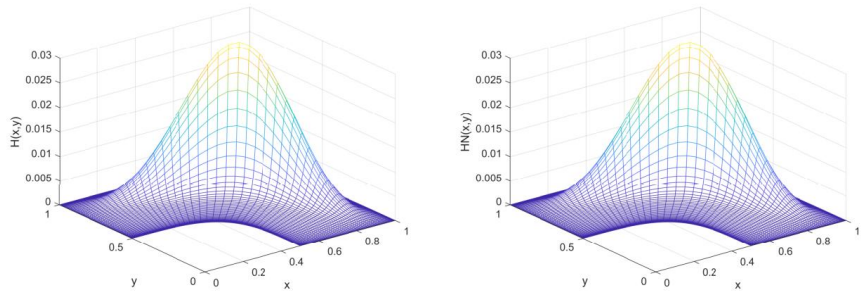

Figure 1: Comparison of the exact solution $H(x,y)$ (left) and approximate solution $H_N(x,y)$ (right) for $N = 30$.

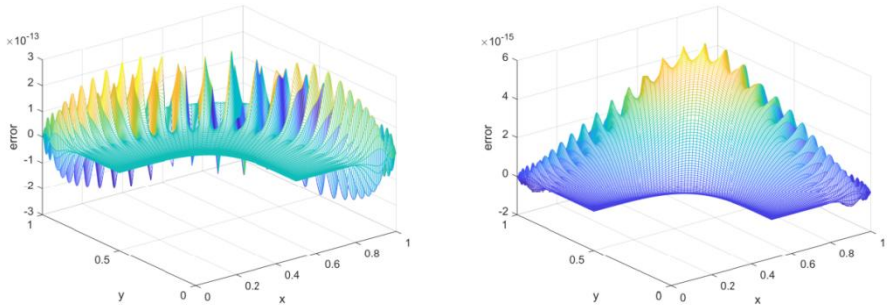

Figure 2: Error images between approximation solutions $H_N(x,y)$ and exact solution $H(x,y)$ for $N = 50$ (left) and $N = 60$ (right).

International Journal of Scientific Engineering and Science
Volume 9, Issue 1, pp. 71-76, 2025. ISSN (Online): 2456-7361

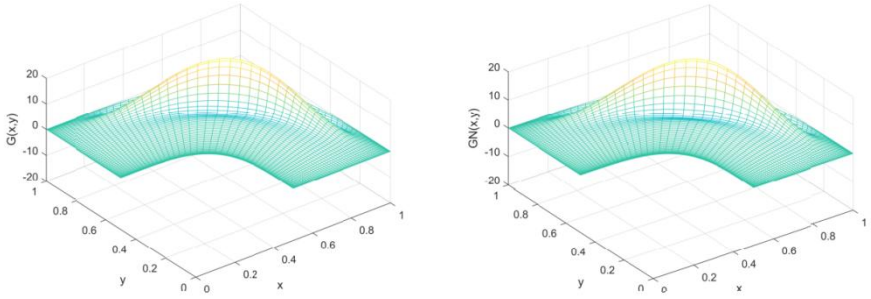

Figure 3: Comparison of the exact solution $G(x,\ y)$ (left) and approximate solution $G_N(x,y)$ (right) for when $N = 30$.

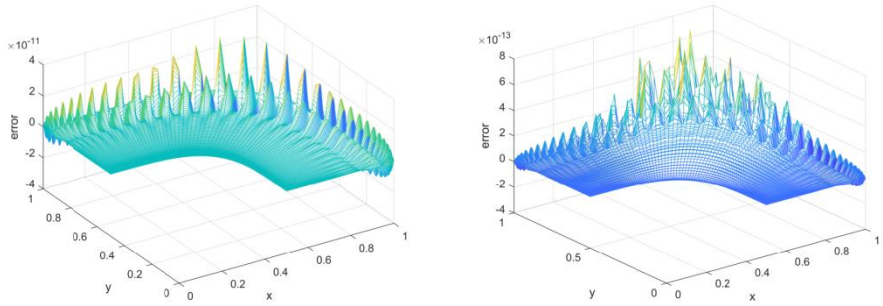

Figure 4: Error images between approximation solutions $G_N(x,y)$ and exact solution $G(x,\ y)$ for $N = 60$ (left) and $N = 70$ (right).

Based on Table 1 and Table 2, it is evident that when $N \geq 60$, the errors between the exact solutions $H(x,y)$ and $G(x,\ y)$ and the approximate solutions $H_N(x,y)$ and $G_N(x,y)$ in these two norms have reached approximately 10^{-15} and 10^{-11} accuracy, respectively. Furthermore, as observed from Figures 1-4, the algorithm demonstrates convergence and spectral accuracy.

Example 2. We take $\alpha = 1,\ \beta = 2,\ \theta_1 = 0,\ \theta_2 = \pi,\ a = \frac{1}{2},\ b = 1$. Let

$$H(x,y) = -e^{x+y}y^3(x^4 + y^4 - \frac{1}{16})^3(x^4 + y^4 - 1)^3.$$

It is evident that $H(x,y)$ satisfies boundary conditions. By substituting $H(x,y)$ into the equation (1), we obtain $F(x,y)$. Similarly, we present the errors between the exact solutions $H(x,y)$ and $G(x,\ y)$ and the approximate solutions $H_N(x,y)$ and $G_N(x,y)$ in Table 3 and Table 4, respectively. Furthermore, the comparison diagrams of the exact solution and the approximate solution are presented in Figures 5 and 7. Meanwhile, the error diagrams between them are presented in Figures 6 and 8.

TABLE 3. For various values of N, the errors between the exact solution $H(x,y)$ and the approximate solution $H_N(x,\ y)$.

N	40	50	60	70	80
$\|H(x,y)-H_N(x,y)\|_{L^2}$	5.3549×10^{-8}	2.7305×10^{-9}	1.3414×10^{-10}	5.0943×10^{-12}	3.0776×10^{-13}
$\|H(x,y)-H_N(x,y)\|_{L^\infty}$	1.1345×10^{-7}	6.6136×10^{-9}	2.6109×10^{-10}	1.1149×10^{-11}	6.4695×10^{-13}

TABLE 4. For various values of N, the errors between the exact solution $G(x,\ y)$ and the approximate solution $G_N(x,y)$.

N	40	50	60	70	80
$\|G(x,y)-G_N(x,y)\|_{L^2}$	1.1762×10^{-4}	7.5937×10^{-6}	5.3934×10^{-7}	2.5851×10^{-8}	1.8328×10^{-9}
$\|G(x,y)-G_N(x,y)\|_{L^\infty}$	4.3103×10^{-4}	2.7951×10^{-5}	2.2306×10^{-6}	1.0839×10^{-7}	7.8479×10^{-9}

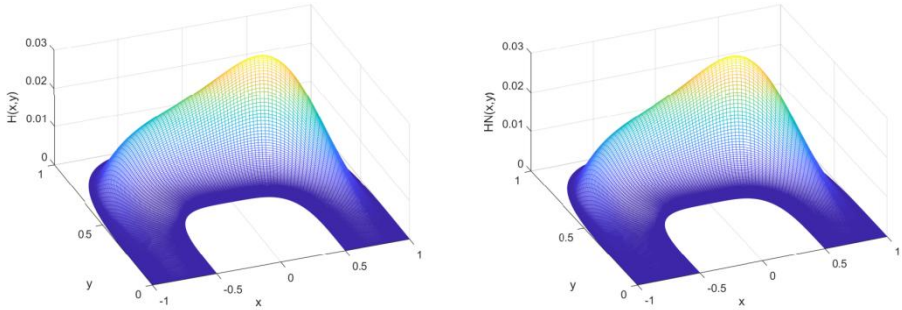

Figure 5. Comparison of the exact solution $H(x,y)$ (left) and approximate solution $H_N(x,\ y)$ (right) for when $N = 80$.

International Journal of Scientific Engineering and Science
Volume 9, Issue 1, pp. 71-76, 2025. ISSN (Online): 2456-7361

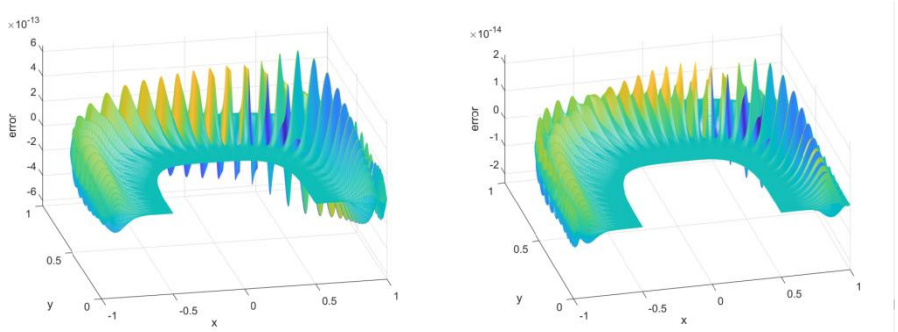

Figure 6: Error images between approximation solutions $H_N(x, y)$ and exact solution $H(x, y)$ for $N = 80$ (left) and $N = 90$ (right).

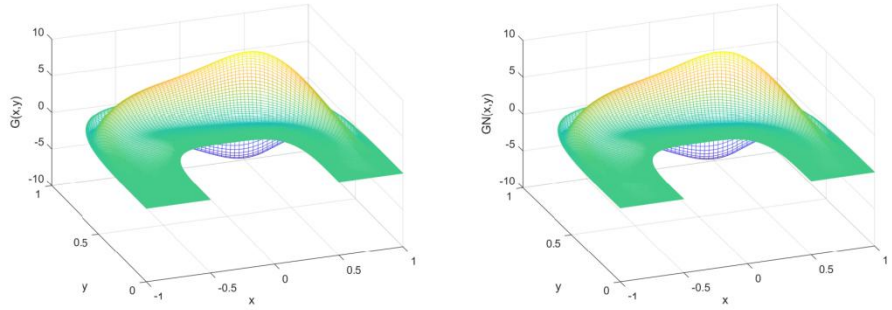

Figure 7: Comparison of the exact solution $G(x, y)$ (left) and approximate solution $G_N(x, y)$ (right) for when $N = 80$.

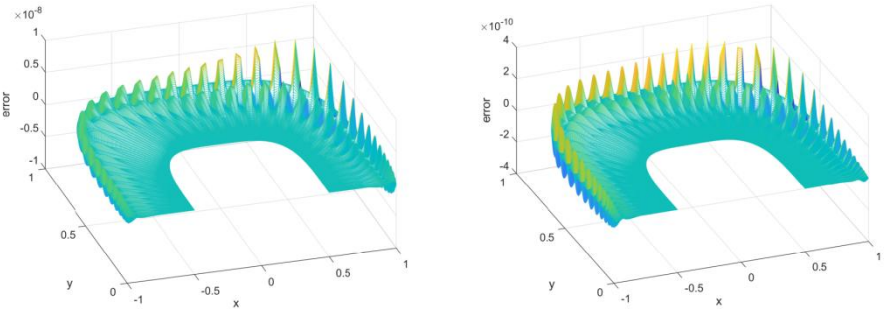

Figure 8: Error images between approximation solutions $G_N(x, y)$ and exact solution $G(x, y)$ for $N = 80$ (left) and $N = 90$ (right).

Based on Table 3 and Table 4, it is evident that when $N \geq 80$, the errors of the exact solutions $H(x, y)$ and $G(x, y)$ and the approximate solutions $H_N(x, y)$ and $G_N(x, y)$ in these two norms have reached approximately 10^{-13} and 10^{-9} accuracy, respectively. Figures 5-8 further demonstrate the stability and convergence of our algorithm.

VI. Conclusion

In this article, we introduce a high-order numerical method for addressing fourth-order problems on complex sectorial domains. The primary approach involves introducing auxiliary variables and formulating an affine transformation. This transformation allows us to transform the fourth-order problem within complex sectorial domains into a second-order coupled system within standard rectangular domains. Subsequently, we establish the corresponding mixed variational formulation and discrete scheme. Furthermore, leveraging the orthogonality of Legendre polynomials, we construct a set of effective basis functions and derive the matrix form of the discrete variational form based on tensor products.

It is noteworthy that the algorithm proposed herein has the potential to be extended to more intricate regions, and this extension serves as our upcoming research objective.

References

[1] You, Y. L., Kaveh, M.Fourth-order partial differential equations for noise removal.IEEE Transactions on Image Processing, 2024 , 9(10): 1723-1730.
[2] Ou, Z. Y.Unbalanced fourth-order interference beyond coherence time.Physical Review Research, 2022, 4(2): 023125.
[3] Whitt, B. Fourth-order gravity as general relativity plus matter. Physics Letters B,1978, 145(3-4): 176-178
[4] Li, L., An, J. An efficient spectral method and rigorous error analysis based on dimension reduction scheme for fourth order problems. Numerical Methods for Partial Differential Equations,2021, 37(1): 152-171.
[5] Cueto-Felgueroso, L., Juanes, R. Adaptive rational spectral methods for the linear stability analysis of nonlinear fourth-order problems. Journal of Computational Physics,2009, 228(17): 6536-6552.
[6] Fei, M., Huang, C. GalerkinCLegendre spectral method for the distributed-order time fractional fourth-order partial differential equation. International Journal of Computer Mathematics, 2020 , 97(6): 1183-1196.
[7] Liu Y, Du Y, Li H, He S, Gao W. Finite difference/finite element method for a nonlinear time-fractional fourth-order reactionCdiffusion problem. Computers Mathematics with Applications., 2015 , 70(4):573-591.
[8] Bayliss A, Jordan KE, LeMesurier BJ, Turkel E.A fourth-order accurate

finite-difference scheme for the computation of elastic waves. Bulletin of the Seismological Society of America, 1986, 76(4):1115-1132.
[9] Wang C, Liu JG, Johnston H. Analysis of a fourth order finite difference method for the incompressible Boussinesq equations. Numerische Mathematik, 2004 , 97:555-594.
[10] Chen H, Guo H, Zhang Z, Zou Q. A linear finite element method for two fourth-order eigenvalue problems. IMA Journal of Numerical Analysis, 2017 , 37(4):2120-2138.
[11] Dupont T, Percell P, Scott R. A family of finite elements with optimal approximation properties for various Galerkin methods for 2nd and 4th order problems. RAIRO.Analyse numrique, 1979, 13(3):227-255.
[12] Liu Y, Fang Z, Li H, He S. A mixed finite element method for a time-fractional fourth-order partial differential equation.Applied Mathematics and Computation, 2014 ,243:703-717.
[13] Pereira JM, Kobayashi MH, Pereira JC. A fourth-order-accurate finite volume compact method for the incompressible NavierCStokes solutions. Journal of Computational Physics, 2001 , 167(1): 217-243.
[14] Felker KG, Stone JM. A fourth-order accurate finite volume method for ideal MHD via upwind constrained transport. Journal of Computational Physics, 2018, 375: 1365-1400.
[15] Wang Z, Wen X, Yao G An efficient spectral-Galerkin method for elliptic equations in 2D complex geometries. Journal of Scientific Computing, 2023, 95(89): 1-26.